Physics Letters B 753 (2016) 449–452

Contents lists available at ScienceDirect

Physics Letters B

www.elsevier.com/locate/physletb

First time evidence of pronounced plateaus right above the Coulomb barrier in ^{8}Li + ^{4}He fusion

A. Del Zoppo *, M. La Cognata

Istituto Nazionale di Fisica Nucleare – Laboratori Nazionali del Sud, via S. Sofia 62, 95123 Catania, Italy

ARTICLE INFO

Article history:
Received 2 October 2015
Received in revised form 11 November 2015
Accepted 17 December 2015
Available online 21 December 2015
Editor: V. Metag

Keywords:
Heavy-ion fusion
Near-barrier cross sections

ABSTRACT

We investigate unprecedented experimental information on the fusion reaction induced by the radioactive projectile ^{8}Li on a ^{4}He gas target, at center-of-mass energies between 0.6 and 5 MeV. The main issue is the tendency of the dimensionless fusion cross section $\frac{\sigma_f}{\pi\lambda^2}$ to form well visible plateaus alternated to steep rises. This finding is likely to be the most genuine consequence of the discrete nature of the intervening angular momenta observed so far in fusion reactions right above the Coulomb barrier. A partial-wave analysis, exclusively based on a pure quantal penetration fusion model and sensitive to the interaction potential, identifies a remarkably low-height barrier.

Nuclear fusion of colliding light ions is a relevant process in many phenomena [1,2]. The fusion cross section of identical doubly-even light nuclei at high center of mass energies sometime signals interesting structures or oscillations attributable to the successive onset of higher partial waves as their centrifugal barriers are exceeded [3–5]. In principle, at energies above the Coulomb barrier, such cross section data should allow a satisfactory immediate determination of the barrier height trend with increasing angular momentum. However, recent detailed descriptions of ^{28}Si+^{28}Si fusion cross section data, such as coupled channel calculation models, rather indicate that the link between the occurrence of an oscillation and the height of the corresponding centrifugal barrier might not be so simple [6]. Thus, attempting a totally different strategic approach is mandatory.

In this context, the behavior of light fusing systems should be investigated. Indeed, in light fusing systems, channel couplings may typically play a less important role. Moreover, very little has been experimentally established so far about the fusion of non-identical light nuclei, lighter than ^{12}C + ^{12}C.

In the domain of possible applications, this kind of investigation could be an interesting and timely issue. The fusion between light ions plays an important role in astrophysical sites such as, for instance, in evolving massive stars, in white dwarf Type Ia supernovae and in surface explosions of neutron stars [7–11]. Light nuclei are utilized in accelerator-based inertial fusion for energy production purposes [12].

In this work, we obtain for the first time experimental information on the fusion of ^{8}Li + ^{4}He → ^{12}B. The choice of this unusual colliding system, because of the radioactive ^{8}Li (τ = 1.21 s), is motivated by the possibility of exploiting the great opportunity provided by the almost total absence of internal bound excitations in both colliding partners.

The fusion cross section σ_f is established at energies E_{cm} = 0.6–5 MeV. It is determined dividing experimentally available ^{11}B + n exit channel data by the corresponding experimentally available branching ratio data.

Regarding the ^{11}B + n exit channel, three independent concordant sets of ^{8}Li + ^{4}He → ^{11}B + n reaction cross section data are identified in [13,14]. We used such three sets of unbiased values to explore the role of exotic cluster structures in [15] and to formulate the recommended cross section in [16]. The resulting analytical expression was adopted in the astrophysical network of [17]. These three experiments can be grouped according to the detected species in: ^{11}B measurements [18,19] and neutron measurement [20,21]. In the ^{11}B measurements [18,19], a 4π multiple sampling ionization chamber (MUSIC) was used as an active gas target. The energy loss along the particle trajectories was measured and the detector thickness was sufficient to span the excitation function with a single beam energy. In the neutron measurement [20,21], a zero-energy-threshold 4π thermalization counter was used in combination with a passive gas target. The counter provided comparable sensitivity to all possible ^{11}B + n branches. Moreover, its characteristic capture time response [22] allowed unambiguous reaction-neutron yield separation even in presence of an intense background level.

* Corresponding author.
E-mail address: DelZoppo@lns.infn.it (A. Del Zoppo).

http://dx.doi.org/10.1016/j.physletb.2015.12.055

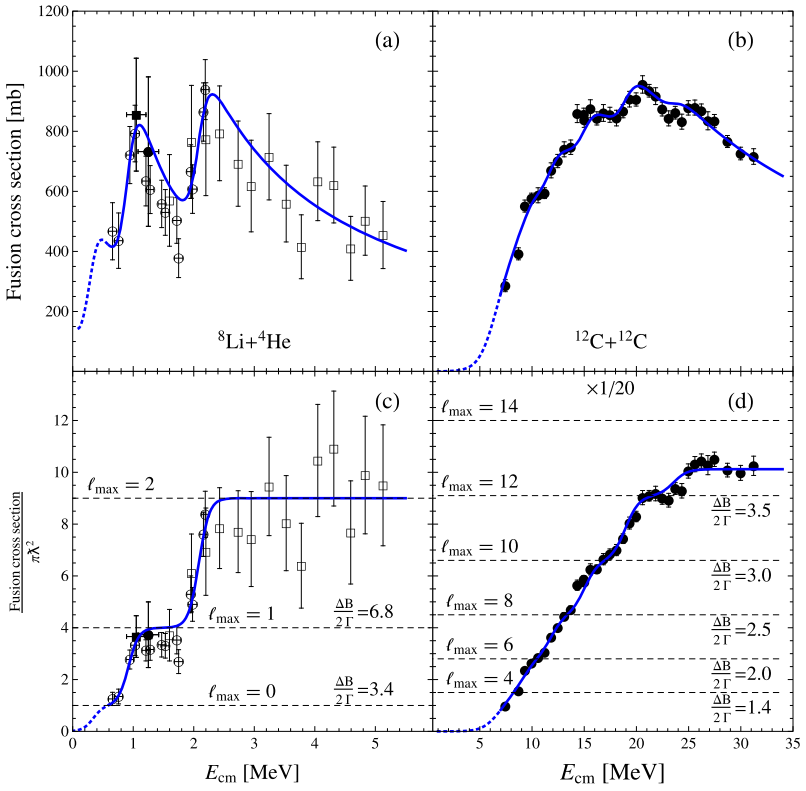

Fig. 1. Left panels: unprecedented experimental information for ^{8}Li + ^{4}He, a) fusion cross section; c) dimensionless cross section. Right panels: experimental information for ^{12}C + ^{12}C, b) fusion cross section [26]; d) dimensionless cross section.
In the left panels, different symbols correspond to the various ^{11}B + n exit channel data sources considered in this work for the evaluation of the fusion cross sections shown in panels a), c): open squares [18], open circles [19], filled circle [20], filled square [21].
In panel d) all ordinates are divided by 20.
The solid curves are the results of the MINUIT data fits described in the text.
The dashed curve in panel c) is the evaluated extrapolation according the adopted formalism.

All three data sets provide the requested ^{8}Li + ^{4}He → ^{11}B + n cross section summed over all ^{11}B final states.

For the sake of completeness we mention the other, exclusive, data set obtained by detecting ^{11}B and neutron coincident signals [23]. Such a set shows smaller cross sections than those considered above [18–21], in the entire energy region. Since there was a significant threshold on the neutron energy, some of the ^{11}B final states could completely escape detection, as discussed in detail in [13]. Therefore, such exclusive measurement cannot provide the cross section summed over all ^{11}B final states at each explored E_{cm}. For this reason, the data set [23] is not suited for the specific aim of this work.

Concerning the experimental branching ratios of the dissociation of the ^{12}B* states into ^{11}B + n, the data given in [24,25] are considered. These branching ratios were obtained via the ^{9}Be$(\alpha, p)^{12}$B* reaction, used to investigate the decay property of states just inside the narrow energy range $E_{cm} = 0.65$–5 MeV of interest here.

The uncertainty caused by the above absolute evaluation of the fusion cross section moderately contributes to the error bars of σ_f only for $E_{cm} > 3$ MeV and up to the conservative upper limit of $E_{cm} \sim 5$ MeV. The resulting fusion cross section data is reported in Fig. 1a as a function of the E_{cm}-values below 5 MeV. The error bars almost exclusively stem from the scarce count statistics caused by the use of the radioactive ^{8}Li projectile, with typical intensity of 10^2–10^3 ions/s.

We remark the sawtooth-like behavior of σ_f versus E_{cm}. However, with the error bars into play, a reliable oscillation analysis of the type in [3], based on the second derivative of the fusion cross section, is impossible. An alternative, more practicable, approach is necessary.

We start by observing that the general trend of this excitation function for ^{8}Li + ^{4}He is considerably different from those in ^{12}C + ^{12}C [26] and ^{16}O + ^{16}O [27]. Previously studied light ion systems exhibit oscillatory structure, with a period of some MeV, in the fusion cross section excitation functions. Fig. 1b shows the ^{12}C + ^{12}C data [26], the literature case where such oscillations are most evident. The comparison of Figs. 1a–b evidences that the peak to valley ratio of these structures is much larger in the case of the ^{8}Li + ^{4}He fusion cross section. Furthermore, such pronounced candidate oscillations appear at somewhat lower energy, around 1–2 MeV, and with a shorter period of only about 1 MeV.

In Figs. 1c–d we show these same fusion data from a different perspective [4]. We consider the dimensionless cross section expressed in units of $\pi\lambda\!\!\!^{-2}$. For ^{8}Li + ^{4}He, the $\frac{\sigma_f}{\pi\lambda\!\!\!^{-2}}$ rises by as much as an order of magnitude with E_{cm} increasing from 0.6 to 2 MeV. However, the rise is not totally monotonic. In fact, two nearly horizontal plateaus clearly alternate with steep rises. The first plateau, between 1 and 1.8 MeV, corresponds to the prominent structure at $E_{cm} \sim 1$ MeV in Fig. 1a. The second plateau, above 2 MeV, extends up to 5 MeV, at least. For comparison, we show in Fig. 1d the dimensionless cross section of the ^{12}C + ^{12}C reaction. With increasing energy, most of the oscillations in σ_f (Fig. 1b) are transformed into more or less increasingly pronounced inflections in $\frac{\sigma_f}{\pi\lambda\!\!\!^{-2}}$ until the two highest oscillations are transformed into nearly horizontal extended plateaus. These two plateaus occur at $E_{cm} > 20$ MeV, at much higher energy with respect to ^{8}Li + ^{4}He.

Previously known oscillatory structures, like those of the $^{12}C + ^{12}C$ cross section in Fig. 1b, plausibly arise from entrance channel effects, likely the progressive addition of higher partial waves with increasing energy, rather than from properties of the compound nuclear system [3–5]. In order to probe such an interpretation in the low energy scenario of the $^{8}Li + ^{4}He$ data, we start considering a formalism of ion–ion fusion that explicitly takes into account the angular momentum of the relative motion l. We assume a sharp angular momentum cut-off that allows all of the flux crossing the interaction barrier to fuse for values of $l \leq l_{max}$. We also consider l_{max} a monotonic increasing discrete function of E_{cm} (see e.g. [28]). Accordingly, the dimensionless cross section is calculated as

$$\frac{\sigma_f}{\pi \lambda\!\!\!^{-2}} = \Delta l \sum_{l=0,\,\Delta l}^{l_{max}} (2l+1) T_l, \tag{1}$$

where $\Delta l = \Delta l_{max} = 1$ for $^{8}Li + ^{4}He$ fusion, whereas $\Delta l = \Delta l_{max} = 2$ for the identical even–even colliding ions case, for which all odd partial waves amplitudes vanish. In Eq. (1), T_l is the energy-dependent penetration probability of the l-th partial wave through the interaction barrier. In particular, when all T_l competing to a given energy tend to unity, more or less pronounced plateaus may appear at the altitudes

$$\frac{\sigma_f}{\pi \lambda\!\!\!^{-2}} \rightarrow (l_{max}+1)^2 \tag{2}$$

for $\Delta l = \Delta l_{max} = 1$ and

$$\frac{\sigma_f}{\pi \lambda\!\!\!^{-2}} \rightarrow (l_{max}+1)(l_{max}+2) \tag{3}$$

for $\Delta l = \Delta l_{max} = 2$.

For $^{12}C + ^{12}C$, the altitudes (3) are drawn as horizontal lines in Fig. 1d. Only the lower plateau at $19 < E_{cm} < 25$ MeV is located at the correct altitude given by the large angular momentum $l_{max} = 12$. For $^{8}Li + ^{4}He$, the altitudes (2) are drawn as horizontal lines in Fig. 1c. Here, by contrast, apparent quantitative agreement is achieved for both the plateaus in the dimensionless cross section. Moreover, these altitudes correspond to much lower angular momenta than those in $^{12}C + ^{12}C$. The first lower plateau is constituted by 25% $l = 0$, 75% $l = 1$, and is located between well separated p-wave and d-wave barrier penetration rises. The other plateau is purely the saturation of all penetrability T_l at 1 for energies well above the highest $l_{max} = 2$ barrier.

It should be noted that the above quantitative characterization of the involved angular momenta is performed regardless of the barrier shape.

Now, we more deeply address our analysis to the barrier shape, for both $^{8}Li + ^{4}He$ and $^{12}C + ^{12}C$. To this purpose, we implement the above analytical model so that barrier parameter values and related uncertainties are simultaneously determined from the data using standard error propagation procedures. Each quantal barrier penetration coefficient T_l is approximated as in [29] by that of an inverted parabolic potential with l-dependent height B_l and intrinsic energy width Γ_l

$$T_l(E_{cm}) = \left[1 + exp\left(\frac{B_l - E_{cm})}{\Gamma_l}\right)\right]^{-1}, \tag{4}$$

the smaller Γ, the steeper the sub-barrier rise of T_l. We also consider that in the non-central collisions (p, d, …-waves) the barrier heights B_l depend linearly on $l(l+1)$, i.e. $B_l = B_0 + \frac{l(l+1)}{2\mathscr{I}}$, where B_0 is the height of the inter-nucleus potential $V(R) = V_C(R) + V_N(R)$ formed in s-wave collisions by the interplay between the repulsive, Coulomb, and the attractive, nuclear, interactions. This is hereafter referred to as the Coulomb barrier. $\mathscr{I}\hbar^{-2}$ is the moment of inertia

Table 1
Barrier height, intrinsic width and moment of inertia parameter sets determined for both reactions using MINUIT data fitting procedure. The radial distances R_{CB} at the Coulomb barrier height, each determined assuming $\mathscr{I} = \mu R_{CB}^2$, μ being the reduced mass, are listed in the last column.

Reaction	B_0 (MeV)	Γ (MeV)	$\mathscr{I}$ (MeV^{-1})	R_{CB} (fm)
$^{8}Li + ^{4}He$	0.34 ± 0.05	0.08 ± 0.02	1.72 ± 0.07	5.2 ± 0.2
$^{12}C + ^{12}C$	5.70 ± 0.12	0.65 ± 0.14	5.88 ± 0.10	6.4 ± 0.11

at the radial distance R_{CB} of the Coulomb barrier height B_0. Last, we set $\Gamma_0 = ... = \Gamma_{l_{max}} = \Gamma$. By inserting (4) into (1), data fit are performed using MINUIT, treating B_0, Γ and $\mathscr{I}$ as free parameters. For $^{12}C + ^{12}C$, good fit is obtained in the whole data range by attenuating the transmission $T_{l=14}$ by a factor $0 < A_{14} < 1$, treated as fourth free parameter, and assuming that all higher partial waves cease to fuse above 20 MeV. The value of $A_{14} = 0.35 \pm 0.05$ is obtained. For $^{8}Li + ^{4}He$, we consider the partial waves up to $l_{max} = 2$, though the onset of a largely attenuated f-wave around 4 MeV cannot be excluded to within the error bars. Below that energy, the semiclassical estimates of the grazing angular momentum l_g coincide with those of l_{max}. In the range above about 4 MeV, $l_g = 3$. The resulting curves are shown in Figs. 1a–d. As an example, for $^{8}Li + ^{4}He$, we find that the agreement in Fig. 1a between the calculated sawtooth and the data behavior is remarkably good. In the sawtooth, each rise is determined by a given steep barrier penetration and each falloff is proportional to $\lambda\!\!\!^{-2} \propto \frac{1}{E_{cm}}$.

The values of the barrier parameters resulting from these data fit are listed in Table 1. We remark that for $^{12}C + ^{12}C$ the barrier parameters values are in agreement with those used in [5]. For the first time, here we give the uncertainties resulting from the data fit.

We now comment on the properties of the resulting $^{8}Li + ^{4}He$ potential.

The value of the radial distance R_{CB} in Table 1 is quite consistent with summed projectile and target radii and with plausible values of the surface diffuseness parameter a of the exponential nuclear potential (see e.g. [5]). In particular a = 0.9 or 0.6 fm, depending on the nucleon radius $r_0 = 1.2$ or 1.3 fm, respectively. The same holds for $^{12}C + ^{12}C$.

Similarly for the intrinsic width Γ. In fact, $\frac{\sigma_f}{\pi \lambda\!\!\!^{-2}}$ (1) is proportional to the energy weighted cross-section $\sigma_f E_{cm}$. The first derivative of (1), using (4), is the weighted sum of l-dependent barrier distributions, each centered at B_l and having width very close to $2\Gamma_l$. Since the width of a typical barrier distribution is proportional to $Z_1 Z_2$ [5], Γ is expected to increases by a factor 6 passing from $^{8}Li + ^{4}He$ to $^{12}C + ^{12}C$, quite consistent with the value of 8.1 ± 2.7 resulting from Table 1.

Instead, the value of the height B_0 captures attention. In this regard, we recall that the experimental data in Fig. 1c seems to indicate the occurrence of a third plateau at the altitude $\frac{\sigma_f}{\pi \lambda\!\!\!^{-2}} = 1$ as expected from (2) for $l_{max} = 0$. Namely, the transmission $T_0 \sim 1$ already at E_{cm} as low as 600 keV. This fact indicates that, actually, $B_0 < 600$ keV and that the available excitation function in Fig. 1a entirely develops above the Coulomb barrier. The fitting procedure does nothing but respond to this trend in the available data. We also recall, that the barrier height $B_0 = V_N(R_{CB}) + V_C(R_{CB})$, R_{CB} being the larger solution of $\frac{d}{dR}[V_N(R) + V_C(R)] = 0$. Namely, no apparent simple scaling of B_0 with projectile and target charges can intuitively be envisaged. Consequently, the large reduction factor in Table 1, ~ 16, relative to $^{12}C + ^{12}C$ might well be plausible, although in absolute the low value of B_0 determined here for $^{8}Li + ^{4}He$ represents a novelty that deserves further insights.

A relevant aspect in this matter is the evaluation of the experimental sensitivity to the fusion barrier and its dependence on the

projectile-target system. In this context, for sure the existence of plateaus in $\frac{\sigma_f}{\pi\lambda^2}$ is of great importance. Because once a well pronounced extended plateau is formed, it acts as a pedestal for the well separated sub-barrier rise of the next entering higher l-wave. If a plateau-rise-plateau alternation is observed, as in Figs. 1c–d, that data portion is primarily and extremely sensitive to the barrier height B_l and width Γ_l. In fact, the barrier height B_l is directly identified to a good approximation by the energy at which the steeply rising data intercepts the half-distance between the two horizontal plateaus; the barrier width Γ is linked to a good approximation to the slope of the rise. The adoption of a fitting procedure, of the type used above, inter alia, also serves to better determine these parameter uncertainties caused by the experimental errors. To quantify both the plateau resolving power and the sensitivity to the barrier shape, we adopt the successive barrier separation to barrier width dimensionless ratio $\frac{\Delta B}{2\Gamma}$ as indicator. We, then, evaluate its values using the parameters in Table 1. In the $^{12}C + {}^{12}C$ ($\Delta l = 2$) reaction case in Fig. 1d eight partial waves are involved. The effects of lower l-waves are barely outlined, when not completely obscured. A barrier sensing plateau-rise-plateau scenario clearly manifests only at $l_{max} = 12$, at center of mass energies as high as 15–20 MeV above the Coulomb barrier B_0. The values $\frac{\Delta B}{2\Gamma} = \frac{2l_{max}+3}{2.\mathscr{I}\Gamma}$, increasing linearly with increasing l_{max}, are reported in Fig. 1d for five of the involved partial waves from $l_{max} = 4$ to $l_{max} = 12$. There, we observe that the transition from inflections to horizontal plateaus, i.e. from low to high sensitivity, takes place for $3 < \frac{\Delta B}{2\Gamma} < 3.5$. The plateau at $l_{max} = 12$ is characterized by $\frac{\Delta B}{2\Gamma} = 3.5$, right at the transitional sensitivity.

For $^{12}C + {}^{12}C$, it seems also instructive the fact that the fitting function extended to energies below 7 MeV, and to $l_{max} < 4$ (dashed segment in Fig. 1b), does not show any type of visible modulation. Hence, one can state with reasonable confidence that, among the structure observed at energies below 7 MeV (see e.g. [30] and references therein), none of those observed right above the fusion barrier, between 5.7 MeV and 7 MeV, should be identified as oscillation with $l_{max} < 4$. In other words, in $^{12}C + {}^{12}C$ fusion data at $E_{cm} < 7$ MeV, the structures right above the barrier should not have the same physical origin of those above 7 MeV in Fig. 1b.

Passing to the $^{8}Li + {}^{4}He$ case in Fig. 1c, we stress once again that only three partial waves, $l = 0$, $l = 1$ and $l = 2$, contribute and that pronounced rise-plateau alternations are clearly observed already at the lower energies. Fig. 1c shows that, in this reaction case, the indicator values $\frac{\Delta B}{2\Gamma} = \frac{l_{max}+1}{4.\mathscr{I}\Gamma}$ amount to at least ~ 3.4, namely both plateau resolution and sensitivity to the barrier shape are significantly large, thanks to both small $\mathscr{I}$ and Γ values. Consequently, in the $^{8}Li + {}^{4}He$ case, it is right the data portion closer to the Coulomb barrier B_0 that imposes the most stringent constraints to the entire excitation function data fit.

To summarize, in this work we obtain unprecedented experimental information on the fusion reaction induced by the radioactive projectile ^{8}Li on a ^{4}He gas target, at center-of-mass energies E_{cm} between 0.6 and 5 MeV, right above the Coulomb barrier. The main issue is the tendency of $\frac{\sigma_f}{\pi\lambda^2}$ to form two well visible plateaus alternated to steep rises. This is the observed fact. In the first instance, we can interpret this observation by a fusion model that solely includes the action of the relative motion angular momentum. The plateau altitudes are found to correspond to the values given by (2) for $l_{max} = 1$ and $l_{max} = 2$, regardless of the fusion barrier shape. If this is the proper description, the clear jump between the undistorted plateau altitudes in the $^{8}Li + {}^{4}He$ data in Fig. 1c is likely to be the most genuine consequence of the discrete nature of the intervening angular momenta observed so far in fusion reactions. Concerning barrier shape determination, for $^{8}Li + {}^{4}He$ neither coupled-channel effects nor collision partner deformations should significantly operate [31]. For $^{12}C + {}^{12}C$, in [3] it was not possible to reproduce well the fusion data in Fig. 1b by coupled channels calculations. Consequently, a pure single barrier penetration fusion model is adopted here for both reactions. Hill-Wheeler barrier penetration formula [29] is used. Most of the barrier parameters determined here for $^{8}Li + {}^{4}He$ fusion are plausibly consistent with those for $^{12}C + {}^{12}C$ fusion. The possible exception is B_0: for $^{8}Li + {}^{4}He$, present work identifies a remarkably low Coulomb barrier that can be possibly linked to the presence of the loosely bound ^{8}Li. This result likely reflects the enhanced sensitivity to the fusion barrier interior using very light systems. It is apparently clear that the Coulomb barrier shape found here for $^{8}Li + {}^{4}He$, if confirmed by further investigations, may provide additional constraints to the nuclear interaction potential in terms of tail slope and/or pocket depth. Further, parallel investigations should also be aimed at evaluating the role of possible nuclear structure induced resonances, an alternative process that does not seem quantitatively supported by the presently available experimental evidences (see e.g. [32]).

In conclusion, this work has shown for the first time the existence of pronounced plateaus right above the Coulomb barrier in $^{8}Li + {}^{4}He$ fusion. These plateaus allow enhanced experimental sensitivity to the fusion barrier given that the most barrier-sensing lowest partial waves are well separated. We expect that the present results for $^{8}Li + {}^{4}He$ will promote further investigations of the fusion reaction mechanism between very light ions at energies much below the interaction barrier. For the moment, we believe that understanding the plateau origin in the cross section above the barrier will almost certainly be useful to corroborate the extrapolation to the important astrophysical region below the Coulomb barrier.

References

[1] B.B. Back, et al., Rev. Mod. Phys. 86 (2014) 317.
[2] L. Canto, et al., Phys. Rep. 596 (2015) 1.
[3] H. Esbensen, Phys. Rev. C 85 (2012) 064611.
[4] C.Y. Wong, Phys. Rev. C 86 (2012) 064603.
[5] N. Rowley, K. Hagino, Phys. Rev. C 91 (2015) 044617.
[6] G. Montagnoli, et al., Phys. Lett. B 746 (2015) 300.
[7] L.R. Gasques, et al., Phys. Rev. C 72 (2005) 025806.
[8] L.R. Gasques, et al., Phys. Rev. C 76 (2007) 035802.
[9] D.G. Yakovlev, et al., Phys. Rev. C 74 (2006) 035803.
[10] L. Buchmann, C.A. Barnes, Nucl. Phys. A 777 (2006) 254.
[11] W.A. Fowler, G.R. Caughlan, B.A. Zimmerman, Annu. Rev. Astron. Astrophys. 13 (1975) 69.
[12] See, for example, Y. Oguri, J. Hasegawa, K. Horioka, S. Kawata, in: Y. Oguri, J. Hasegawa, K. Horioka, S. Kawata (Eds.), Proceedings of the 17th International Symposium on Heavy Ion Inertial Fusion, Tokyo, Japan, 2008, Nucl. Instrum. Methods A 606 (2009) 1.
[13] M. La Cognata, et al., Astrophys. J. Lett. 706 (2009) L251.
[14] M. La Cognata, et al., J. Phys. G, Nucl. Part. Phys. 37 (2010) 105105.
[15] M. La Cognata, A. Del Zoppo, Phys. Scr. T 150 (2012) 014019.
[16] M. La Cognata, A. Del Zoppo, Astrophys. J. 736 (2011) 148.
[17] A. Coc, et al., Astrophys. J. 744 (2012) 158.
[18] R.N. Boyd, et al., Phys. Rev. Lett. 68 (1992) 1283.
[19] X. Gu, et al., Phys. Lett. B 343 (1995) 31.
[20] S. Cherubini, et al., Eur. Phys. J. A 20 (2004) 355.
[21] M. La Cognata, et al., Phys. Lett. B 664 (2008) 157.
[22] A. Del Zoppo, et al., Nucl. Instrum. Methods A 581 (2007) 783.
[23] H. Ishiyama, et al., Phys. Lett. B 640 (2006) 82.
[24] S. Kubono, et al., Z. Phys. A 341 (1991) 121.
[25] Z.Q. Mao, et al., Nucl. Phys. A 567 (1994) 125.
[26] D.G. Kovar, et al., Phys. Rev. C 20 (1979) 1305.
[27] I. Tserruya, et al., Phys. Rev. C 18 (1978) 1688.
[28] D. Glas, U. Mosel, Nucl. Phys. A 237 (1975) 429.
[29] D.L. Hill, J.A. Wheeler, Phys. Rev. 89 (1953) 1102.
[30] T. Spillane, et al., Phys. Rev. Lett. 98 (2007) 122501.
[31] K. Hagino, N. Takigawa, Prog. Theor. Phys. 128 (2012) 1061.
[32] G. Domogala, H. Freiesleen, Nucl. Phys. A 467 (1987) 149.